Electronic supplementary information

Biomass Derived N/C-catalyst for Electrochemical Production of Hydrogen Peroxide

Yiran Yang, Fei He, Yanfei Shen, Xinghua Chen, Hao Mei, Songqin Liu and Yuanjian Zhang*

Jiangsu Engineering Laboratory of Smart Carbon-Rich Materials and Device, Jiangsu Province Hi-Tech Key Laboratory for Bio-Medical Rresearch, School of Chemistry and Chemical Engineering, Medical School, Southeast University, Nanjing 211189, China

Email: Yuanjian.Zhang@seu.edu.cn

Experimental section

Chemical and materials: Pomelo was purchased from Orient Fruit Industry (Fujian, China). Ultrapure Water (18.2 MΩ cm) was acquired from a Smart2 water purification system (Thermal, USA). Unless otherwise specified, all chemicals and solvents were purchased from Sinopharm Chemical Reagent Co., Ltd or Aladdin Chemistry Co., Ltd. and were of analytical reagents and used without further purification.

Preparation of N-doped carbon from pomelo peel: The general process to prepare N-doped carbon is shown in Figure S1. Briefly, the soft and white part of pomelo peel was extracted and cut into small pieces and freeze-dried for a week. As a control, 1.0 g of pomelo peel powder was stirred with 50 ml of ethanol solution containing 0.48 g of ferric chloride hexahydrate ($FeCl_3 \cdot 6H_2O$, 99%) at room temperature for 24 hours (the mass ratio of Fe in pomelo peel powder precursor was 10%). Then, ethanol was removed via rotary evaporation and the as-obtained composite was dried for 10 hours at 80 ^oC under vacuum. Both of these two precursors were pyrolyzed at 900 ^oC for 1 hour in N_2 at a heat rate of 10 ^oC min^{-1}. Thereafter, the as-prepared products were ground to powder, and stirred with 20 ml of 37 wt% HCl at room temperature overnight to remove unstable species. The final catalysts (denoted as N/C-900 and Fe-N/C-900, respectively) were obtained by centrifuge, washed with water, ethanol, diethyl ether in sequence and dried in vacuum at 80 ^oC for 12 hours.

The Fe (ferric chloride) was chosen as a precursor to control the influence of defects towards ORR evaluation. It was because there were many reports using Fe ions in the preparation of N-doped carbon for ORR (e.g. Ref 23: Dai et al., *Science*, 2009, 323, 760). It was generally supposed that Fe species would catalyze the graphitization process during the high temperature carbonization. Hence, normally at the same carbonization temperature, the N-doped carbon that was prepared using Fe ions would have a high degree of graphitization, i.e., less disorder carbonous defect. Moreover, as chlorine ions can easily combine with protons to produce volatile hydrogen chloride gases, it would help the removal of counter anions of Fe ions.

As controls, pomelo peel-derived N-doped carbon with and without Fe species at different annealing temperature, i.e., 800, 900 and 950 ^{o}C was also prepared (the mass ratio of Fe in pomelo peel powder precursor was 10%) in a similar way. The obtained samples was named as Fe-N/C-T-10% and N/C-T, respectively, where T represent the pyrolysis temperature.

Moreover, to understand the influence of Fe content on the graphitization and catalytic H_2O_2 production performances, pomelo peel-derived N-doped carbon with different amount of Fe were also synthesized at 900 ^{o}C in a similar way. The mass ratio of Fe in pomelo peel precursors was 5%, 10%, and 15%, respectively. The as-prepared samples were named as Fe-N/C-900-5%, Fe-N/C-900-10%, and Fe-N/C-900-15%, respectively.

It should be noted that since the influence of Fe content on the graphitization and catalytic H_2O_2 production performances was not comprehensively discussed in the main text, Fe-N/C-900-10% was also named as Fe-N/C-900 in the main text for short.

Electrochemical measurement: The evaluation of electrocatalytic H_2O_2 generation activity by various N/C catalysts was carried out on a standard three-electrode system on CHI700E workstation (CH Instruments, USA). Pt wire and commercially Ag/AgCl (saturated KCl, E(RHE)=0.196+E(Ag/AgCl)+0.0592×pH) were used as the counter and reference, respectively. All electrochemical tests were performed in 0.1 M KOH, and the reliability of Ag/AgCl in our experimental conditions were verified by the same results via exploring calomel electrode as the reference. The steps of preparation of working electrodes were as follows: the pre-polished rotating glassy carbon electrode (3 mm diameter) or rotating ring-disk electrode (4 mm diameter) was uniformly drop-cast with 4 mg mL^{-1} catalyst ink, leading to a catalyst loading of 566 μg cm^{-2}. After that, the electrode was dried in air at 60 ^{o}C for 15 min. Then, it was further modified with 5 μL of Nafion (0.05 wt%), and dried in air at 60 ^{o}C for 15 min. For H_2O_2 generation, high purity O_2 gas was passed into the electrolyte for 30 min. Cyclic voltammetry (CV) was used to measure redox properties of catalysts. Linear sweep voltammetry (LSV) was used to measure ORR activity of catalysts,

which was performed at a rotating electrode (RRDE-3A, BAS, Japan). To determine yield of H_2O_2, ring potential was set to 1.4656 V (versus RHE) to oxidize H_2O_2 transferred from glassy carbon disk electrode. Yield of H_2O_2, electron transfer number (n) and Faraday efficiency (%) were calculated by following equations (Miner et al., *Nat. Commun.* 2016, 7, 10942; Antoine et al., *J. Appl. Eletrochem.* 2000, 30, 839):

$$H_2O_2(\%) = 200 \times \frac{\frac{I_R}{N_0}}{\left(\frac{I_R}{N_0}\right)+I_D} \quad (1)$$

$$\mathrm{n} = 4 \times \frac{I_D}{\left(\frac{I_R}{N_0}\right)+I_D} \quad (2)$$

$$\text{Faraday efficiency}\ (\%) = \frac{\left(\frac{I_R}{N_0}\right)}{I_D} \quad (3)$$

where I_D and I_R are disk and ring currents, respectively, and N_0 is ring collection efficiency. The value of N_0 was determined to be 0.42 in a solution containing 5 mM $K_4Fe(CN)_6$ + 5 mM $K_3Fe(CN)_6$.

The Koutecky-Levich equation (equation 4) was used to calculate electron transfer number (n) according to the experimental data of RDE.

$$\frac{1}{J} = \frac{1}{J_K} + \frac{1}{J_L} = \frac{1}{J_K} + \frac{1}{B\omega^{1/2}} \quad (4)$$

$$\mathrm{B} = 0.62\mathrm{nF}C_o(D_o)^{\frac{2}{3}}v^{-\frac{1}{6}} \quad (5)$$

$$J_k = nFkC_o \quad (6)$$

in which J is the measured current density, J_K and J_L are the kinetic and diffustion-limiting current densities, ω is the angular velocity of the rotating electrode ($\omega = 2\pi N$, where N is the linear speed of rotation), n is the electron transfer number in the ORR, F is the Faraday constant (96485 C/mol), C_o is the concentration of O_2, D_o is the diffusion coefficient of O_2, v is the kinematic viscosity of the electrolyte, and k is rate constant for electron transfer. According to the electrolyte which was O_2-saturated 0.1 M KOH, the values of C_o, D_o and v were 1.2×10^{-3} M, 1.9×10^{-5} cm^2/s, and 0.01 cm^2/s, respectively (He et al., *J. Mater. Chem. A.* 2016, 4, 6630).

In order to obtain the concentration of H_2O_2 during the electrocatalytic production, ring of RRDE, Pt wire and commercially Ag/AgCl was used as working, counter, and reference electrode, respectively. The calibration curve of current and concentration of H_2O_2 were used to calculate the concentration of H_2O_2 that was produced in electrocatalysis. For this purpose, 0.1 M KOH was pre-saturated with O_2 for 30 min. Then, 10 μl of H_2O_2 of different concentrations were quickly added into the electrolyte. After that, bulk electrolysis with coulometry (Electrolysis E=1.4656 V versus RHE) was applied, and the stable current (I_D') was recorded.

Characterization: Scanning electron microscopy (SEM) was carried out on Ultra Plus field emission electron microscope (Zeiss, Germany). Transmission electron microscopy (TEM) was recorded on JEM-2100 transmission electron microscopy (JEOL, Japan). The surface area was calculated by Brunauer-Emmett-Teller (BET) method according to nitrogen adsorption-desorption isotherms conducted on a NoveWin 1000e instrument (Quantachrome, USA). FT-IR spectra were performed with a NLCOLET iS10 FTIR spectrometer (Thermo Fisher SCIENTIFIC, USA), equipped with and attenuated total reflection (ATR) setup. UV-vis spectra were carried out with Cary 100 UV-vis spectrophotometer (Agilent, Singapore) equipped with a diffuse-reflectance accessory, and $BaSO_4$ was used as the reference sample (100% reflectance). X-ray diffraction (XRD) was performed with a Ultima IV combined multi-functional level X-ray diffractometer (Rigaku, Japan). Raman spectra were carried out on a laser Raman microscope (λ=532 nm, HORIBA JOBIN YVON, France). X-ray photoelectron spectroscopy (XPS) were carried out on a ESCALAB 250Xi spectrometer (Thermo Fisher Scientific, USA) using monochromated Al Kα X-rays at hv=1486.6 eV. The binding energy was calibrated with C 1s of 284.6 eV.

The calculation of W_{parct}: the reaction of oxygen by accepting two electrons in different pH electrolyte conditions was different (W. M. Haynes, *Handbook of Chemistry and Physics*, CRC Press, Boca Raton, 2014).

$$O_2 + 2H^+ + 2e^- \rightarrow H_2O_2 \quad E^\theta$$=0.695 V (vs SHE)

$$O_2 + H_2O + 2e^- \rightarrow HO_2^- + OH^-\ \ E^\theta$$=-0.076 V (vs SHE)

The conversion formula between standard hydrogen electrode and reversible hydrogen electrode was as follows:

E^θ(vs RHE)= E^θ(vs SHE)+0.0592×pH (7)

Here, pH is the initial pH value of the electrolyte.

W was used to evaluate the amount of energy consumption considering the overpotential and Faraday current efficiency in the actual production process.

$$W = \frac{z \times F \times (E^\theta(vs\ RHE) - E(vs\ RHE))}{Faraday\ efficiency} \quad (8)$$

In which, z is the transferred electron number of the reaction, i.e. 2. F is the Faraday constant (96500 C/mol). E(vs RHE) is the actual voltage applied during electrolysis. E^θ(vs RHE) is the standard electrode potential that the reaction can occur. (E^θ(vs RHE)-E(vs RHE)) indicates the value of over potential. Faraday efficiency is also refers to current efficiency.

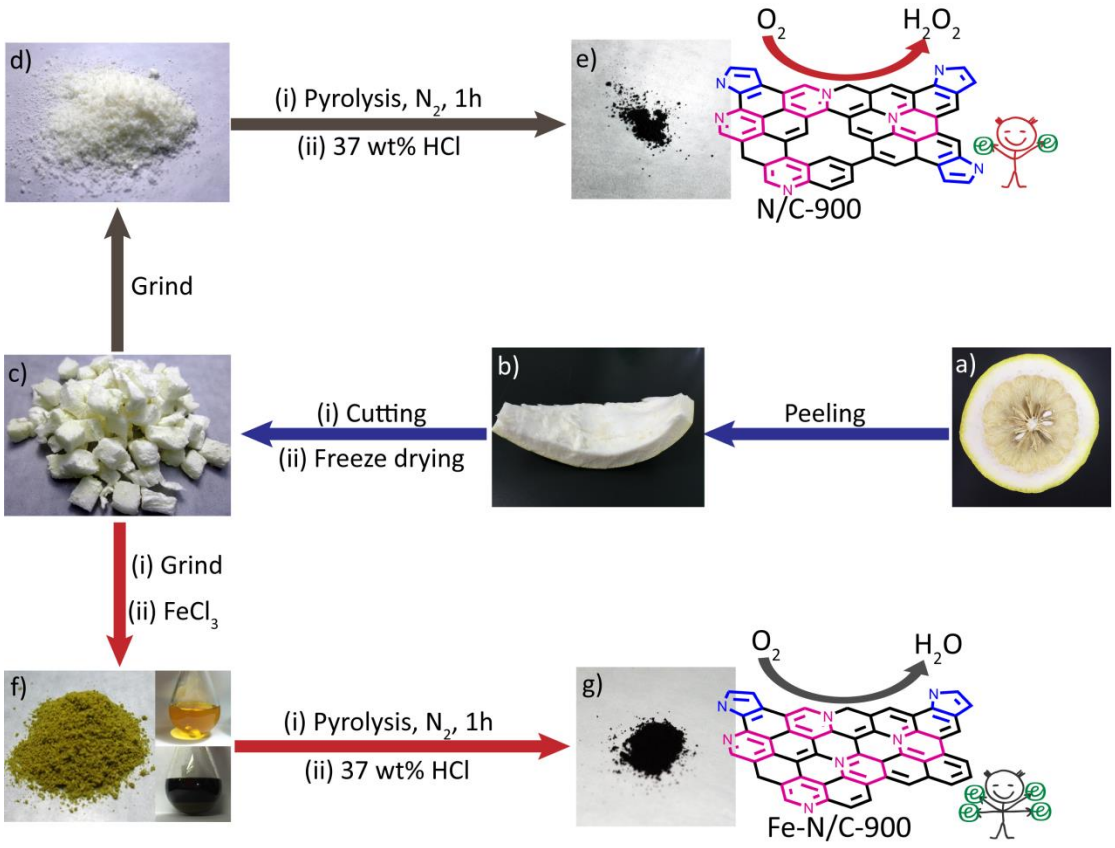

Figure S1 The general procedure for fabricating doped carbon catalysts from pomelo peel. The photo of the pomelo (a), the pomelo peel (b), freeze-dried pomelo peel pieces (c), freeze-dried pomelo peel powder (d), N/C-900 (e), Fe^{3+}-impregnated freeze-dried pomelo peel powder. (f), Fe-N/C-900 (g). Inset in (f) showed the ethanol solution of ferric chloride before (top) and after (bottom) the addition of freeze-dried pomelo peel powder.

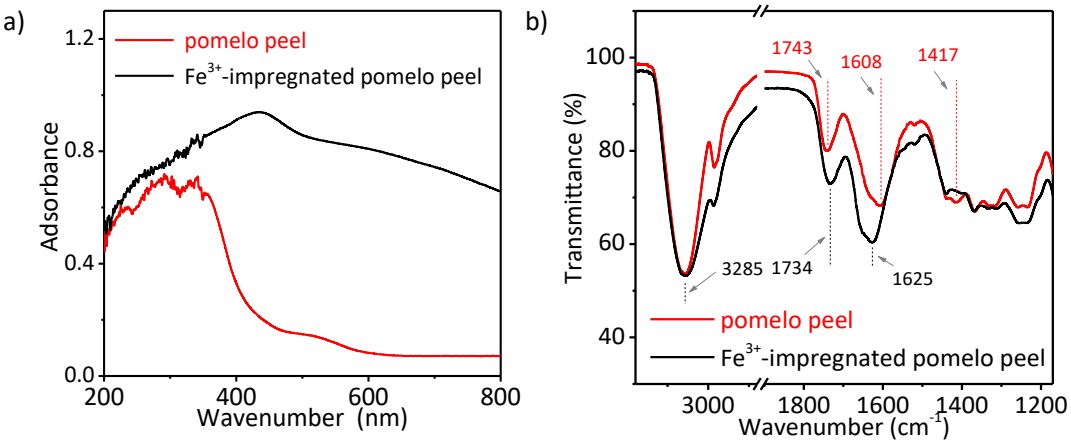

Figure S2 UV-Vis adsorption (a) and FT-IR spectra (b) of freeze-dried pomelo peel powder with and without impregnating of $FeCl_3$.

The UV-vis adsorption spectra (Fig. S2a) and FT-IR spectra (Fig. S2b) of freeze-dried pomelo peel with and without impregnating of $FeCl_3$, indicated its polyhydroxyl nature and the ability of complexation with transition metal ions (R. Gnanasambandam et al., *Food Chem*. 2000, 68, 327).

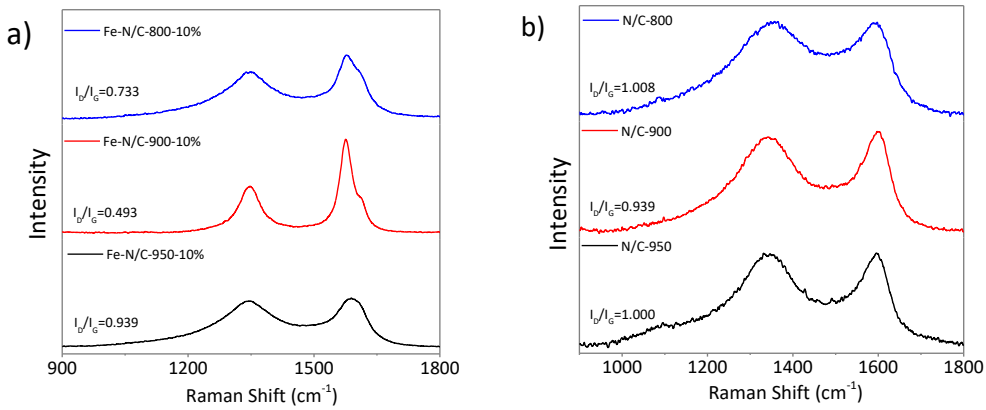

Figure S3 Raman spectra of (a) Fe-N/C-800-10%, Fe-N/C-900-10% and Fe-N/C-950-10% and (b) N/C-800, N/C-900 and N/C-950.

The pomelo peel-derived N-doped carbon with and without Fe species was also prepared at different annealing temperature, i.e., 800, 900 and 950 ^{o}C. In general, the G band occurs at ca. 1600 cm^{-1} because of an E_{2g} hexagonal graphitic lattice, whereas the D band at ca. 1300 cm^{-1} corresponds to the A_{1g} mode of sp^3 carbon. As shown in Fig. S3, these two typical Raman peaks were found for all the samples. To evaluate the graphitic degree, the D band to G band intensity ratio (I_D/I_G) of them was calculated. It can be seen that the I_D/I_G of Fe-N/C-900-10% (0.493) was less than that of Fe-N/C-800-10% (0.733) and Fe-N/C-950-10% (0.939). The I_D/I_G of N/C-900 (0.939) was less than that of N/C-950 (1.000) and N/C-800 (1.008). Thus, the pyrolysis temperature had a significant influence on the graphitization degree of the final catalysts.

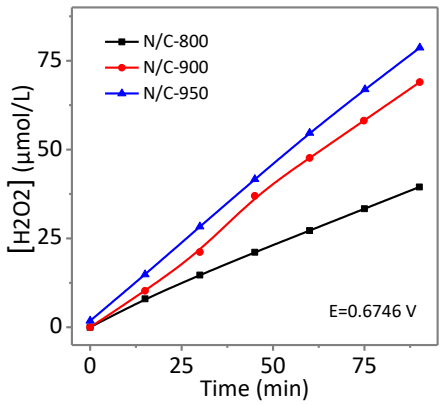

Figure S4 Plot of the amount of peroxide produced over time by N/C-800, N/C-900 and N/C-950.

The performance of N/C-800, N/C-900, N/C-950 in catalytic H_2O_2 production were showed in Figure S4. It was found that the H_2O_2 production rate of N/C-800 (12.6 $g/g_{[cata]}{\cdot}h{\cdot}L$) was the poorest and that of N/C-950 (25.1 $g/g_{[cata]}{\cdot}h{\cdot}L$) was slightly higher than that of N/C-900 (22.0 $g/g_{[cata]}{\cdot}h{\cdot}L$). However, of note, the yield of N/C-950 (3.7%) was much lower than that of N/C-900 (13%), due to significant mass loss by an elevated pyrolysis temperature. In these regards, N/C-900 could be the best candidate for catalytic H_2O_2 production in practical applications.

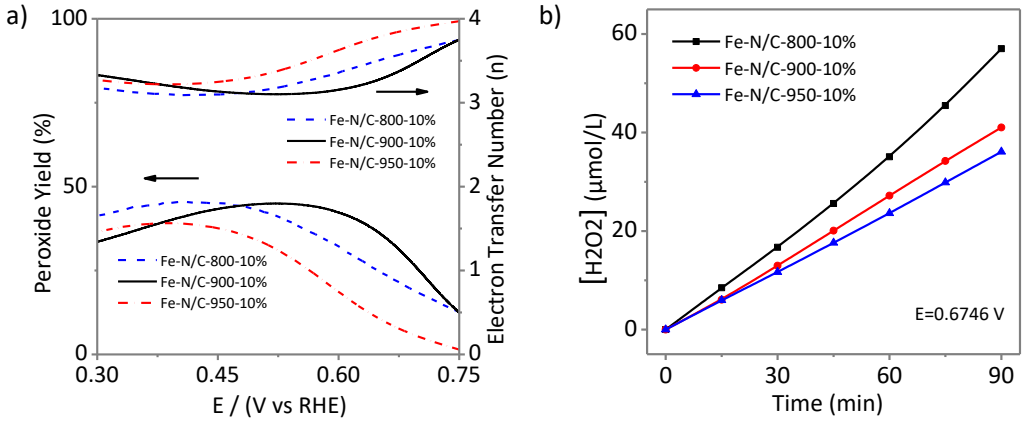

Figure S5 a) Peroxide yield and electron transfer number (n) obtained from RRDE curves for Fe-N/C-800-10%, Fe-N/C-900-10% and Fe-N/C-950-10%. b) Plot of the amount of peroxide produced over time by Fe-N/C-800-10%, Fe-N/C-900-10% and Fe-N/C-950-10%.

The performance of Fe-N/C-800-10%, Fe-N/C-900-10% and Fe-N/C-950-10% in catalytic H_2O_2 production were also measured and showed in Fig. S5. It was found that the electron transfer number (n) of both Fe-N/C-800-10% and Fe-N/C-950-10% were larger than that of Fe-N/C-900-10% and all of them were larger than 3, especially at low overpotential region (0.60-0.75 V vs. RHE), demonstrating that those three samples were not favor of the catalytic H_2O_2 production. Moreover, the H_2O_2 production rate of them was evaluated, and it was found the best one was poorer than that of N/C-900.

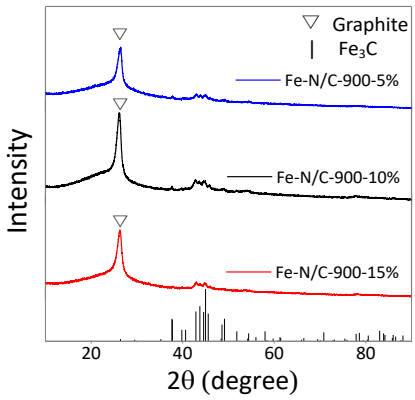

Figure S6 XRD pattern of Fe-N/C-900-5%, Fe-N/C-900-10% and Fe-N/C-900-15%.

To check the extent of graphitization with relevance to $FeCl_3$ content, we have synthesized N-doped carbon with different Fe content. Depending on the Fe mass ratio that was added in the pomelo peel precursor, the three samples was named as Fe-N/C-900-5%, Fe-N/C-900-10%, Fe-N/C-900-15%, in which 900 means the pyrolysis temperature of 900 ^{o}C. XRD measurements were carried out to investigate the extent of graphitization of three samples. As shown Figure S6, the increase of Fe content did not significantly narrow the full width at half maximum (FWHM) of the graphitic carbon 002 peak, located at 26.2^{O}. Thus, the degree of graphitization of the materials did not have a close relationship with the content of $FeCl_3$ in the current study.

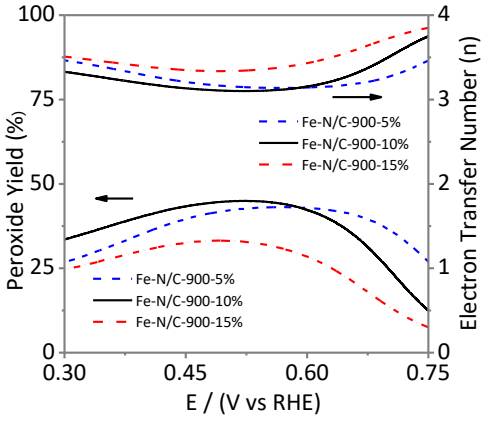

Figure S7 Peroxide yield and electron transfer number (n) obtained from RRDE curves for Fe-N/C-900-5%, Fe-N/C-900-10% and Fe-N/C-900-15%.

The performance of Fe-N/C-900-5%, Fe-N/C-900-10% and Fe-N/C-900-15% in catalytic H_2O_2 production were also measured and showed in Fig. S7. It was found that the electron transfer number (n) of them varied but were all larger than 3, especially at low overpotential region (0.60-0.75 V vs. RHE), demonstrating that those three samples were not favor of the catalytic H_2O_2 production.

a) b)

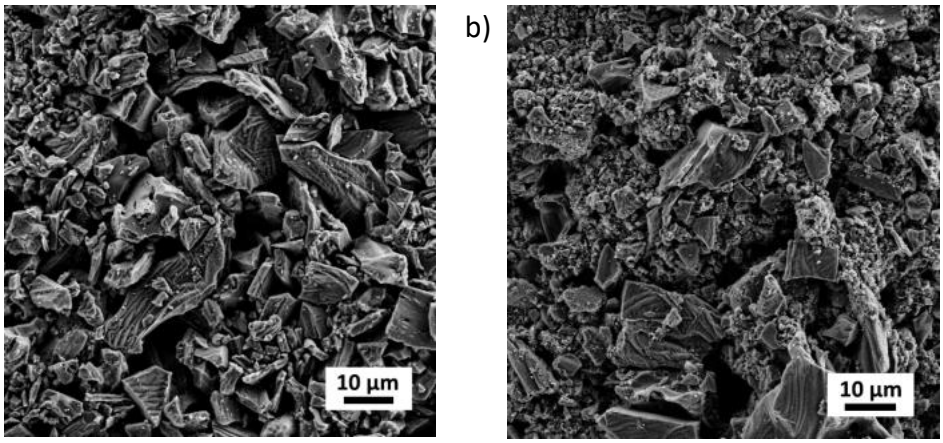

Figure S8 SEM image of N/C-900 (a) and Fe-N/C-900 (b).

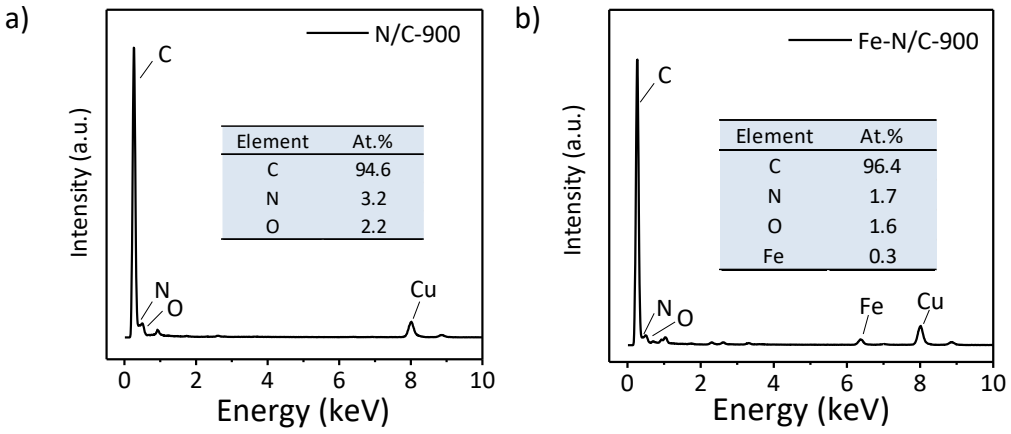

Figure S9 EDS of N/C-900 (a) and Fe-N/C-900 (b).

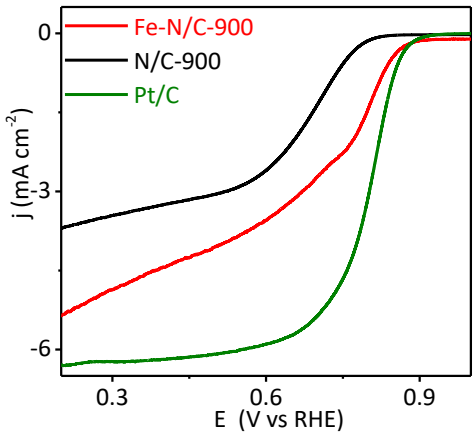

Figure S10 RDE LSV curves for N/C-900, Fe-N/C-900 and Pt/C in 0.1 M KOH at a scan rate of 10 mV s^{-1} and a rotation speed of 1600 rpm.

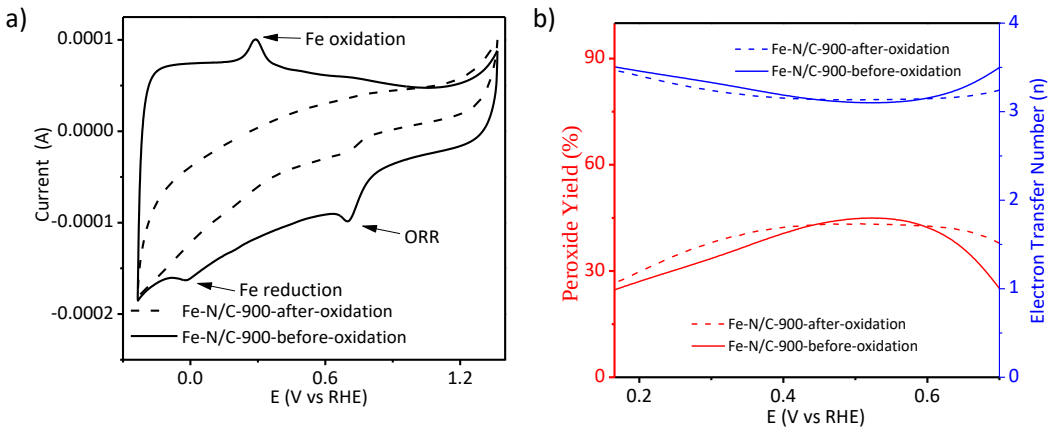

Figure S11 (a) CV curves of Fe-N/C-900 before and after electrochemical oxidation etching of Fe_3C. Scan rate: 50 mV s^{-1}. (b) Electron transfer number (n) and peroxide yield obtained from RRDE curves for Fe-N/C-900 before and after electrochemical oxidation etching of of Fe_3C. Scan rate: 10 mV s^{-1}.

In order to eliminate the interfere coming from Fe_3C in Fe-N/C-900 in terms of the selectivity of the catalyst for the ORR, we purified Fe-N/C-900 by electrochemical oxidation in phosphate buffer (pH=6.8) at a potential of 2.3656 V (vs RHE) for 236 s (Gong et al., *Science.* 2009, 323, 760). Next, potential sweeping from 1.3656 V ~ -0.2344 V in 0.1 M KOH was performed subsequently until a stable cyclic voltammetry was achieved which were showed in Figure S11a. It was clearly that the peaks of Fe reduction and Fe oxidation were disappeared after electrochemical oxidation etching, while Fe-N/C-900's catalytic properties (the selectivity of ORR) of ORR were not changed significantly (the electron transfer number in the whole potential region was ca. 3-3.5, Figure S11b). It indicated that Fe_3C in Fe-N/C-900 did not evidently contribute the selectivity for the ORR.

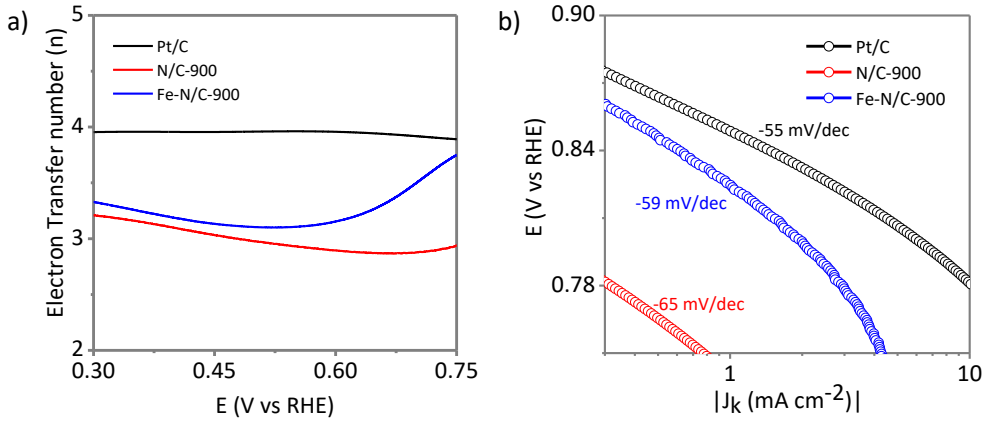

Figure S12 (a) The electron transfer number (n) and (b) Tafel plots of N/C-900, Fe-N/C-900, and Pt/C.

The electron transfer number (n) throughout the potential window and Tafel plots for N/C-900, Fe-N/C-900 and Pt/C has been added into the revised ESI as Figure S12, which was consisted with the hydrogen peroxide yield in Figure 4c. The Tafel slope of N/C-900 and Fe-N/C-900 were -65 mv/dec and -59 mV/dec respectively, close to the -55 mV/dec for the Pt/C catalyst, indicating the transfer of the first electron catalyzed by N/C-900 and Fe-N/C-900 were possibly the rate-determining step (Li et al., *Nat. Nanotechnol*. 2012, 7, 394).

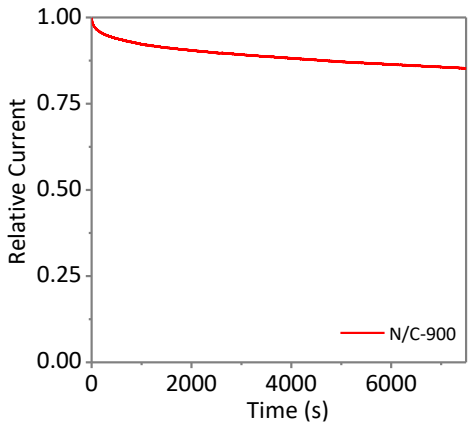

Figure S13 Chronoamperometry curve of N/C-900 for stability test. Biased potential: 0.5656 V vs. RHE.

The stability of N/C-900 in catalytic H_2O_2 production was tested by chronoamperometry. As shown below, the catalytic current retained up to 85% in 6000 s, indicating its high stability in electrolysis.

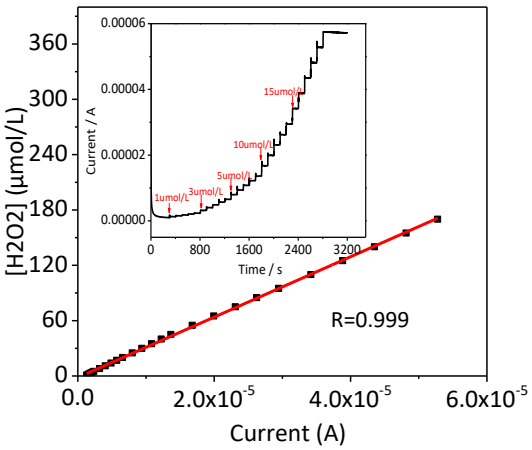

Figure S14 Amperometric response at Pt electrode to successive addition of H_2O_2 and the calibration curve. The Pt electrode was biased at 1.4656 V (vs RHE) and rotated at 1600 rpm in 0.1 M KOH.

Table S1 Summary of the elemental atom ratio of different-typed C and N in N/C-900 and Fe-N/C-900 from XPS.

	C (at.%)		N (at.%)		O (at.%)		Fe (at.%)	
N/C-900	graphitic C	74.64	pyrrolic N	0.52				
	C-N	8.21	pyridinic N	0.42				
	C-O	7.30	graphitic N	0.56				
			oxidized N^+-O^-	0.26				
	C_{total}	90.15	N_{total}	1.76	O_{total}	8.09	Fe_{total}	0
Fe-N/C-900	graphitic C	79.89	pyrrolic N	0.24				
	C-N	8.79	pyridinic N	0.32				
	C-O	4.87	graphitic N	0.39				
			oxidized N^+-O^-	0.21				
	C_{total}	93.55	N_{total}	1.16	O_{total}	4.97	Fe_{total}	0.33

Table S2 The comparison of catalyst performance among the reference samples and N/C-900.

Sample names	pH	E (vs RHE)	$[H_2O_2]$ $g/(g_{[cata]}\cdot h)$	$[H_2O_2]$ $g/(g_{[cata]}\cdot h\cdot L$	Efficiency (%)	W[a] $W\cdot h/g_{[H2O2]}$	Refs
Mesoporous nitrogen-doped carbon	1	0.1	-	54.69	65.15	1.58	6a
Hierarchically porous carbon	1	0.2 0	5.7902 9.996	289.51 499.8	85.2 91.2	1.025 1.304	6b
AC/VGCF/PTFE	7	0.3104	-	15.32	31	4.06	7b
Rolling carbon black/ PTFE	3	-	-	1.89	-	-	7h
Co-carbon composite catalysts	0	0.25	0.17	-	80	0.877	7c
Quinone and riboflavin catalysts/ Vulacan XC72 carbon	0	0.1	-	2.1	70	1.34	7d
Carbon nanotube	5.99	0.24	-	-	40	3.19	7e
		0.0512	-	5.4	-	-	
Ni3(hexaiminotriphenylene)$_2$	13	0.55 0.65	5.266	-	63 63	0.359 0.109	7f
Carbon fiber coated mesh substrate	7	0.5104	-	0.9	52	1.816	7g
N/C-900	13	0.6746 0.55 0.5 0.3	1.688 - - -	22.0 - - -	39.5 36.5 34.4 24.6	0.076 0.620 0.887 2.52	This work

[a] W means the energy consumption for generation of 1 g H_2O_2.